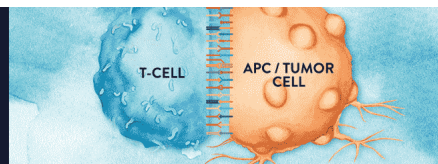


Ultra-pure antibodies for
in vivo research, targeting
immune checkpoints
and more.

EXPLORE



This information is current as
of February 19, 2021.

Simultaneous Presence of Non- and Highly Mutated Keyhole Limpet Hemocyanin (KLH)-Specific Plasmablasts Early after Primary KLH Immunization Suggests Cross-Reactive Memory B Cell Activation

Claudia Giesecke, Tim Meyer, Pawel Durek, Jochen Maul, Jan Preiß, Joannes F. M. Jacobs, Andreas Thiel, Andreas Radbruch, Reiner Ullrich and Thomas Dörner

J Immunol 2018; 200:3981-3992; Prepublished online 7 May 2018;

doi: 10.4049/jimmunol.1701728

<http://www.jimmunol.org/content/200/12/3981>

Supplementary Material

<http://www.jimmunol.org/content/suppl/2018/05/05/jimmunol.1701728.DCSupplemental>

References

This article **cites 63 articles**, 26 of which you can access for free at:
<http://www.jimmunol.org/content/200/12/3981.full#ref-list-1>

Why *The JI*? [Submit online.](#)

- **Rapid Reviews! 30 days*** from submission to initial decision
- **No Triage!** Every submission reviewed by practicing scientists
- **Fast Publication!** 4 weeks from acceptance to publication

**average*

Subscription

Information about subscribing to *The Journal of Immunology* is online at:
<http://jimmunol.org/subscription>

Permissions

Submit copyright permission requests at:
<http://www.aai.org/About/Publications/JI/copyright.html>

Email Alerts

Receive free email-alerts when new articles cite this article. Sign up at:
<http://jimmunol.org/alerts>

The Journal of Immunology is published twice each month by
The American Association of Immunologists, Inc.,
1451 Rockville Pike, Suite 650, Rockville, MD 20852
Copyright © 2018 by The American Association of
Immunologists, Inc. All rights reserved.
Print ISSN: 0022-1767 Online ISSN: 1550-6606.



Simultaneous Presence of Non- and Highly Mutated Keyhole Limpet Hemocyanin (KLH)-Specific Plasmablasts Early after Primary KLH Immunization Suggests Cross-Reactive Memory B Cell Activation

Claudia Giesecke,^{*,†} Tim Meyer,[‡] Pawel Durek,^{*} Jochen Maul,^{‡,§} Jan Preiß,[‡] Joannes F. M. Jacobs,[¶] Andreas Thiel,^{||} Andreas Radbruch,^{*} Reiner Ullrich,[‡] and Thomas Dörner^{*,#}

There are currently limited insights into the progression of human primary humoral immunity despite numerous studies in experimental models. In this study, we analyzed a primary and related secondary parenteral keyhole limpet hemocyanin (KLH) immunization in five human adults. The primary challenge elicited discordant KLH-specific serum and blood effector B cell responses (i.e., dominant serum KLH-specific IgG and IgM levels versus dominant KLH-specific IgA plasmablast frequencies). Single-cell IgH sequencing revealed early appearance of highly (>15 mutations) mutated circulating KLH-specific plasmablasts 2 wk after primary KLH immunization, with simultaneous KLH-specific plasmablasts carrying non- and low-mutated IgH sequences. The data suggest that the highly mutated cells might originate from cross-reactive memory B cells (mBCs) rather than from the naive B cell repertoire, consistent with previous reported mutation rates and the presence of KLH-reactive mBCs in naive vaccinees prior to immunization. Whereas upon secondary immunization, serum Ab response kinetics and plasmablast mutation loads suggested the exclusive reactivation of KLH-specific mBCs, we, however, detected only little clonal overlap between the peripheral KLH-specific secondary plasmablast IgH repertoire and the primary plasmablast and mBC repertoire, respectively. Our data provide novel mechanistic insights into human humoral immune responses and suggest that primary KLH immunization recruits both naive B cells and cross-reactive mBCs, whereas secondary challenge exclusively recruits from a memory repertoire, with little clonal overlap with the primary response. *The Journal of Immunology*, 2018, 200: 3981–3992.

The diversity and clonality of the Ig receptor repertoire affects the quality, kinetics, and effectiveness of primary as well as secondary humoral immune responses. Theoretically, the human Ig BCR repertoire comprises up to 10^{11} unique variants (1). The balance between a highly diverse repertoire of naive B cells versus selected memory B cells (mBCs) and plasma cells, respectively, is key to protect against new and secondary pathogenic challenges. Ag-specific activated naive B cells partly differentiate into short-lived plasma cells secreting low-affinity Abs. Additionally, some of these activated naive B cells found germinal centers (GCs), which give rise to mBCs as well as to

long-lived plasma cells. These plasma cells and the mBC both contribute to a sustained humoral immune memory. An important characteristic of this humoral immunity is the progressive increase in affinity of specific Abs over time following Ag encounter, termed affinity maturation (2, 3). Various studies provided evidence that GCs are the primary sites of Ag-specific B cell affinity maturation (4–8). These studies, mainly performed in rodents, found that as B cells proliferate in the dark zone of the GC, present after 3–4 d upon challenge, they acquire somatic mutations in their Ig V region (V) genes, causing random changes in the BCR sequences that affect their affinity (9–13). Subsequently,

^{*}Zellbiologie, Deutsches Rheuma-Forschungszentrum, ein Institut der Leibniz-Gemeinschaft, 10117 Berlin, Germany; [†]Berlin-Brandenburg School for Regenerative Therapies, Charité Universitätsmedizin Berlin, 13353 Berlin, Germany; [‡]Klinik für Gastroenterologie, Infektiologie und Rheumatologie, Charité Universitätsmedizin Berlin, 12203 Berlin, Germany; [§]Gastroenterologie am Bayerischen Platz, 10825 Berlin, Germany; [¶]Department of Laboratory Medicine, Laboratory Medical Immunology, Radboud University Nijmegen Medical Center, 6525 Nijmegen, the Netherlands; ^{||}Regenerative Immunology and Aging, Berlin-Brandenburg Center for Regenerative Therapies, 13353 Berlin, Germany; and [#]Medizinische Klinik mit Schwerpunkt Rheumatologie und Klinische Immunologie, Charité Universitätsmedizin Berlin, 10117 Berlin, Germany

ORCID: 0000-0002-6179-0670 (P.D.); 0000-0002-1323-0150 (J.M.); 0000-0002-0901-1422 (J.P.); 0000-0002-6208-6386 (J.F.M.J.).

Received for publication December 12, 2017. Accepted for publication April 13, 2018.

This work was supported by Deutsche Forschungsgemeinschaft (DFG) single projects Do491/7-3, Do491/10-1, and DFG SFB 633/A14 and DFG funding through Berlin-Brandenburg School for Regenerative Therapies GSC 203.

C.G. and T.D. designed the study and wrote the manuscript. C.G. designed and performed experiments, analyzed data, and prepared figures. C.G. and P.D. performed statistical analyses. T.M., J.M., J.P., and R.U. were involved in donor recruitment and

sample preparation and helped revise the manuscript. J.F.M.J. performed experiments and helped revise the manuscript. A.T. and A.R. provided scientific advice and helped to revise the manuscript.

The sequences presented in this article have been submitted to the DNA Data Bank of Japan, to the European Molecular Biology Laboratory, and to GenBank under accession numbers MH167588–MH167922.

Address correspondence and reprint requests to Prof. Thomas Dörner or Dr. Claudia Giesecke, Medizinische Klinik mit Schwerpunkt Rheumatologie und Klinische Immunologie, Charité Universitätsmedizin Berlin and Deutsches Rheuma-Forschungszentrum, Charitéplatz 1, 10117 Berlin, Germany (T.D.) or Deutsches Rheuma-Forschungszentrum, Charitéplatz 1, 10117 Berlin, Germany (C.G.). E-mail addresses: thomas.doerner@charite.de (T.D.) or giesecke@drfz.de (C.G.)

The online version of this article contains supplemental material.

Abbreviations used in this article: $\alpha 1$, IgA1 constant H chain; C γ , IgG constant H chain; CDRH3, H chain complementarity-determining region 3; FWR, framework region; GC, germinal center; HD, healthy donor; i.d., intradermally; KLH, keyhole limpet hemocyanin; mBC, memory B cell; R, replacement; S, silent; V, V region.

Copyright © 2018 by The American Association of Immunologists, Inc. 0022-1767/18/\$35.00

the B cells test their BCRs' affinity in the light zone of GCs, where they also undergo class-switch recombination. Selective expansion of clones expressing BCR variants with increased Ag binding occurs, whereas low-binding clones are deleted. This fine-tuned iterative process is expected to result in a specific B cell repertoire with increased affinity based on increased hypermutated BCR rearrangements, with expansion of specific clones within the mBC and plasmablast pool over time. However, early studies in the 1980s performed in rodents demonstrated that secondary and tertiary immune responses largely recalled sequences not dominant or even not present in the primary response, a phenomenon referred to as "repertoire shift" (10, 14, 15). Knowledge about patterns and the nature of the sequential acquisition of somatic hypermutation and clonal selection of specific B cell clones during a primary response into the mBC pool, as well as information about which B cell clones are then recruited in the course of secondary challenges in humans, is lacking. This might be due to the fact that most common immune challenges in human adults (infections or vaccinations) activate preexisting immunity generated in multiple rounds of vaccinations or natural challenges with pathogens. Only young children undergo various defined primary immunizations. However, their young age usually excludes the possibility to sample large amounts of blood for a detailed molecular analysis of directly purified Ag-specific B cells. Thus, the dimensions to which the human mBC repertoire is maintained and reactivates clonal lineages that were employed during primary immunization or infection as well as its subsequent maturation and evolution has not been thoroughly addressed.

In this study, we used parenteral keyhole limpet hemocyanin (KLH) immunization to investigate the kinetics of KLH-specific B cells as well as the magnitude and IgH repertoire quality during a primary and corresponding secondary human B cell response. KLH is a neo-antigen and suitable to study human T cell-dependent primary responses (16), and prior exposure or sensitization is extremely unlikely (17). Although we demonstrate unique specific B cell repertoires in the five individuals studied, distinct common signatures were observed in all adult donors. First, in four of five naive donors, we detected KLH-binding mBCs before immunization, whereas plasmablast and Ab kinetics after immunization resembled that of primary immune responses in all vaccinees (18, 19). Secondly, the serological KLH-specific IgA-to-IgG ratio was distinct from the circulating KLH-specific plasmablast IgA-to-IgG sequence ratio. Thirdly, single-cell sequence analysis revealed that one third of the primary KLH-specific plasmablasts expressed highly mutated IgH V sequences (>15 bp per IgH V region), whereas the other rearrangements exhibited low or unmutated IgH sequences, as expected. Lastly, repertoire analysis within individual donors further demonstrated substantial clonal overlap between different sample days within the primary KLH-specific plasmablast pool but largely lacked clonal relationships with KLH-specific mBC or secondary plasmablast repertoires. The results of our study provide innovative insights into a hitherto underappreciated mechanism of a human primary B cell immune response by the experienced human immune system in which the B cell response to novel Ags may simultaneously employ naive B cells but also cross-reactive B cell clones from an otherwise established memory repertoire; this strategy appears to be economically sensible.

Materials and Methods

Study participants and KLH immunizations

Five healthy donors (HD) (four female and one male, with ages ranging from 27 to 54 y) were immunized with KLH (biosyn, Fellbach, Germany). Donors received a parenteral immunization of either 0.1 mg KLH s.c. (HD2 and HD3), 0.6 mg KLH s.c. (HD1), or 0.5 mg KLH s.c. and 0.5 mg

KLH intradermally (i.d.) (HD4 and HD5). A booster was injected 7 (HD4 and HD5) or 10 d (HD1–HD3) afterward with 1 mg s.c. or 0.1 mg s.c., respectively. Donors HD1, HD2, and HD3 received a secondary immunization 6 mo (HD2 and HD3; 0.01 mg s.c.) or 18 mo (HD1; 0.1 mg s.c.) after primary immunization. EDTA and serum blood (Vacutainer tubes; BD Biosciences, San Jose, CA) were obtained at baseline and at defined time points after immunizations as mentioned below. The study has been approved by the ethics committee of the Landesgesundheitsamt Berlin, and informed consent was obtained by the individuals of this study.

Cell isolation and serum separation

PBMC were isolated from fresh EDTA blood by density gradient centrifugation using Ficoll-Paque PLUS (GE Healthcare Bio-Sciences AB, Uppsala, Sweden) following the manufacturer's instructions. For serum collection, serum blood was centrifuged at $1500 \times g$ for 10 min. Serum was stored at -21°C until further use.

ELISA for detection of KLH-specific serum Abs

KLH-specific Abs were measured in the sera of patients before and after vaccination by ELISA. Briefly, microtiter plates (96 wells; Nunc, Roskilde, Denmark) were coated overnight at 4°C with KLH (25 $\mu\text{g}/\text{ml}$ in PBS per well; biosyn). After washing the plates, the patient's serum was added in duplicate and in two different dilutions (1:50 and 1:150) for 1 h at room temperature. After extensive washing, KLH-specific Abs were detected with mouse anti-human IgG, IgA, or IgM Abs labeled with HRP (Invitrogen, San Diego, CA). 3,3', 5,5'-tetramethyl-benzidine was used as a substrate (Dako, Glostrup, Denmark), and plates were measured in a microtiter plate reader at 450 nm. For quantification, an isotype-specific calibration curve for the KLH response was included in each microtiter plate, as described before (20).

Flow cytometry

For flow cytometric analyses, the following fluorochrome-labeled Abs were used: anti-CD19–allophycocyanin–H7 (allophycocyanin–H7, clone SJ25C1; BD); anti-CD27–allophycocyanin, anti-CD27–PE, or anti-CD27 FITC (FITC; clone L128; BD); anti-CD3–Pacific Blue (clone UCHT1; BD); anti-CD14–Pacific Blue (clone M5E2; BD); and anti-CD20–Pacific Orange (clone HI47; Invitrogen, Frederick, MD). mBCs were defined as $\text{CD}3^{-}\text{CD}14^{-}\text{CD}19^{+}\text{CD}20^{+}\text{CD}27^{+}$ cells and plasmablasts as $\text{CD}3^{-}\text{CD}14^{-}\text{CD}19^{+}\text{CD}20^{-/\text{low}}\text{CD}27^{\text{high}}$ cells. KLH-specific B cells were identified by binding to the immunizing KLH either labeled to cyanine 5 or to digoxigenin (both conjugated at the Deutsches Rheuma-Forschungszentrum), and the latter followed by staining with anti-digoxigenin-FITC (Roche Diagnostics, Mannheim, Germany). The gating strategy is shown in Supplemental Fig. 1A. The specificity of staining was confirmed each time by corresponding blocking with unconjugated KLH (a representative example is shown in Supplemental Fig. 1B). Stainings were performed in the dark at 4°C for 15 min, followed by washing in PBS/1% BSA at $200 \times g$ for 5 min. PBMC were analyzed using a FACSCanto II flow cytometer (BD).

KLH-specific ELISPOT

A KLH-specific ELISPOT was performed to confirm that the direct KLH staining of B cells could identify Ag-specific cells. Therefore, KLH-binding and nonbinding Ab-secreting cells (i.e., plasmablasts), gated as described above, as well as bulk plasmablasts were isolated from HD2 and HD3 on day 16 by FACS and subsequently seeded on a KLH-specific ELISPOT (Supplemental Fig. 1C). Therefore, prior to cell seeding, a MultiScreen flat-bottom 96-well plate (Millipore MAIPN4550; Merck Millipore, Ireland) was prepared by 1 min prewetting with 35% ethanol (Carl Roth, Karlsruhe, Germany), followed by washing with PBS and 1 h incubation with 50 $\mu\text{l}/\text{well}$ of 0.04 mg/ml KLH at 37°C , followed by blocking with PBS/3% BSA. As controls, non-KLH wells were incubated with either undiluted human serum (positive control) or with PBS/3% BSA (negative control). The plasmablast populations isolated by FACS were seeded onto the plate and incubated overnight in RPMI 1640 medium (Life Technologies, NY) supplemented with 10% FCS (Life Technologies) and 1% penicillin/streptomycin (Life Technologies) at $37^{\circ}\text{C}/5\% \text{CO}_2$. Cells were removed by thorough washing with PBS/1% BSA/0.05% Tween 20 (Sigma-Aldrich, Munich, Germany). For detection of secreted KLH-specific Abs, a mix of biotinylated anti-IgA (BD Biosciences), anti-IgM, and anti-IgG (both Sigma-Aldrich) was added in a 1:200 PBS dilution for 1 h at room temperature followed by thorough washing. Spots were visualized by incubation with streptavidin–HRP (Sigma-Aldrich) diluted 1:3000 in PBS, followed by washing and incubation with 3-amino-9-ethylcarbazole (Sigma-Aldrich) dissolved in N,N-dimethylformamide (Sigma-Aldrich) and diluted in a 0.2 M sodium acetate/0.2 M acetic

acid buffer. Plates were analyzed by using an ELISPOT reader (AID; Autoimmun Diagnostika, Strassberg, Germany).

Single-cell PCR for IgH sequence analysis

PBMC were stained as described above, and KLH-specific plasmablasts or mBCs were sorted into a 96-well plate (Greiner Bio-One, Frickenhausen, Germany), with one cell per well, using a FACSaria II cell sorter (BD). Each well contained 30 μ l of a mix for cell lysis and RNA stabilization consisting of 8.3 mM DTT (component of the Titan One Tube RT-PCR system; Roche Diagnostics), 0.5 μ g BSA, 1.7% Triton X-100, 0.8 nM spermidine (in-house preparation), and 20 U RNasin Plus RNase Inhibitor (Promega, WI). Afterwards, a second mix was added containing the Titan One Tube RT-PCR Kit's buffer and avian myeloblastosis virus reverse transcriptase, prepared according to the manufacturer's instructions and supplemented with 0.5 mM deoxyribonucleotide triphosphate (Sigma-Aldrich) and a p(dT)15 primer (Roche). cDNA was generated at 50°C for 60 min. Amplification of rearranged V_HDJ_HC_μ/α_μ transcripts was carried out by nested PCR using 5 μ l of the cDNA, followed by product purification and sequencing as described before (21). Oligonucleotide sequences of V_H1–V_H6 region forward primer sets as well as of the reverse isotype-specific IgA, IgG, and IgM primer sets were as reported previously (22, 23). Five microliters of the external PCR products were used as a template for the internal PCR. Sequences were analyzed as described before (21). The yield for KLH-specific plasmablasts was 299 sequences from 434 sorted cells (68.9%). From 176 sorted KLH-specific mBCs we could recover 36 sequences (20.5%). These sequences are available from DNA Data Bank of Japan, European Molecular Biology Laboratory, and GenBank under accession numbers MH167588–MH167922 (<https://www.ncbi.nlm.nih.gov/genbank/>).

Data analysis

Flow cytometric data were analyzed using FlowJo software 7.6.5 (Tree Star, Ashland, OR) or FACSDiva software (BD). IgH sequences were analyzed using the Chromas 2.33 sequence viewer (Chromas Technology, Helensvale, Australia) and the JOINSOLVER software (link <http://joinsolver.niaid.nih.gov>; kabat database; accessed between May 2012 and June 2014) (24). GraphPad Prism version 5 for Windows (GraphPad Software, San Diego, CA) and Microsoft Excel 2010 (Santa Rosa, CA) were used for further analyses. Mutation patterns were analyzed as described before (21). To estimate the variety of KLH-specific clones, a statistical analysis of the theoretical repertoire sizes was carried out as described (21, 25). This analysis yields a 95% one-sided confidence-bound n , whereby n is the theoretical statistical calculated quantity of different clones within one individual to ensure that the empirical found numbers of observed distinct sequences among all of the examined sequences fit. The probability for the occurrence of at least the particular number of mutations was estimated applying a Poisson distribution model, assuming the independency of each mutation and not considering possible back mutations, or a lag phase, with λ being the product of the mutation rate (r), the number of divisions, and the sequence length for a particular clone. Cells were assumed to divide continuously, with division times of 8 h.

Results

Simultaneous increase of KLH-specific IgM, IgA, and IgG Abs upon primary KLH immunization

Prior to immunization, KLH-specific IgM, IgA, and IgG Ab titers were either below or just above the assay's detection level in all five volunteers hitherto unexposed to KLH (Fig. 1A). After parenteral KLH immunization, KLH-specific Ab titers remained unchanged until day 14. Interestingly, thereafter, specific Abs of all three major isotypes showed a simultaneous increase. Thus, appearance of specific IgM Abs did not precede that of IgA or IgG. KLH-specific IgA and IgG Ab levels both showed a strong increase (i.e., 2- to 32- and 2- to 12-fold, respectively), yet specific IgA Ab levels remained below that of specific IgG Abs. Taken together, primary KLH immunization in adults induced a simultaneous appearance of specific serum Ab of all three isotypes after 2 wk.

Appearance of primary KLH-specific plasmablasts precedes that of KLH-specific mBCs

To investigate the kinetics and quality of the B cell response to KLH immunization, we monitored KLH-specific B cell subsets in

peripheral blood by direct staining and analyzed their IgH sequences after single-cell sorting. Specificity of the direct staining of B cells using fluorochrome-labeled KLH was controlled by block with unlabeled KLH (Supplemental Fig. 1B) as well as by a KLH-specific ELISPOT of FACS-sorted primary KLH-specific plasmablasts (Supplemental Fig. 1C).

KLH-specific plasmablasts were detected at increased frequencies in blood from day 7 on and remained detectable to at least day 21 or 24 after primary immunization (Fig. 1B). In detail, in HD1 (receiving 0.6 mg KLH s.c.), KLH-specific plasmablasts were detectable between day 7 and 21. The cells remained rather stable between day 7 and 10 but increased 44-fold from day 10 to day 14, which also constitutes their peak appearance (17.7% of total plasmablasts). In HD2 and HD3 (receiving 0.1 mg KLH s.c.), KLH-specific plasmablasts were observed at day 10 and remained detectable until day 24, peaking on day 16 (4.6% [HD2] and 6.1% [HD3]). In HD4 and HD5 (receiving 1 mg KLH s.c. and i.d.), KLH-specific plasmablasts were found to be increased at day 7 and showed a further 1.3- to 5-fold increase at day 14 (17.3% [HD4] and 17.2% [HD5]). As already detected among the other donors, circulating KLH-specific plasmablasts were still detectable at day 24 (last time point sampled). Thus, specific plasmablasts induced by primary KLH immunization were continuously detectable in peripheral blood from day 7 on for at least 3 wk with a peak at around 2 wk, together with a trend for a quantitative relationship between vaccination dose and KLH plasmablast and Ig response (Fig. 1).

The kinetics of KLH-specific mBCs differed from that of KLH-specific plasmablasts. In four out of five donors, KLH-specific mBCs were detectable already before immunization (Fig. 1B, right graph). Because in all these donors KLH-specific serum Abs were almost undetectable, we concluded that all donors were immunologically truly naive with respect to KLH, as expected: none of these donors reported previous KLH exposures. Interestingly, KLH binding to these mBCs could only be poorly blocked by preincubation with unlabeled Ag in contrast to the efficient blocking of KLH-binding mBCs at later time points (Fig. 1C). Compared to day 0, KLH-binding mBCs were reduced to absent at day 7 and/or 10 (HD2–HD5) and reappeared afterward (i.e., at day 14 [HD4 and HD5] or a later time point [HD1–HD3]; Fig. 1B). Finally, KLH-specific mBCs peaked between days 18 (HD1, HD4, and HD5) and 21 (HD2 and HD3), which was in all cases later than the corresponding KLH-specific plasmablast peak. Our data show that primary Ag-specific plasmablasts once present in blood show prolonged presence instead of a limited peak. In contrast, the presence of mBCs fluctuates with a pattern suggesting their temporary retention in secondary lymphoid organs, as has been suggested before (26, 27).

Persistence of humoral immunity after primary KLH immunization

To determine how KLH-specific humoral memory is maintained after primary immunization, we analyzed three of the five donors after 18 mo (HD1) or 6 mo (HD2 and HD3). Circulating KLH-specific plasmablasts were absent in contrast to KLH-specific mBCs, which were readily detectable, ranging from 0.084 to 1.76% of all mBCs (data not shown). Whereas anti-KLH IgM Abs were low (just above the assay's detection level), anti-KLH IgG Abs were still detectable at 20–40 mg/l (equivalent to a 2.0- to 6.0-fold level above initial baseline serum levels) but reduced compared with the last time point after their corresponding primary immunization (Fig. 1D). Notably, anti-KLH IgA was also still detectable at levels 1.2- to 12-fold above the initial baseline serum levels. These findings indicate that primary KLH immunization can induce humoral immune memory, including KLH-specific long-lived plasma cells that produce persistent specific serum IgA and IgG

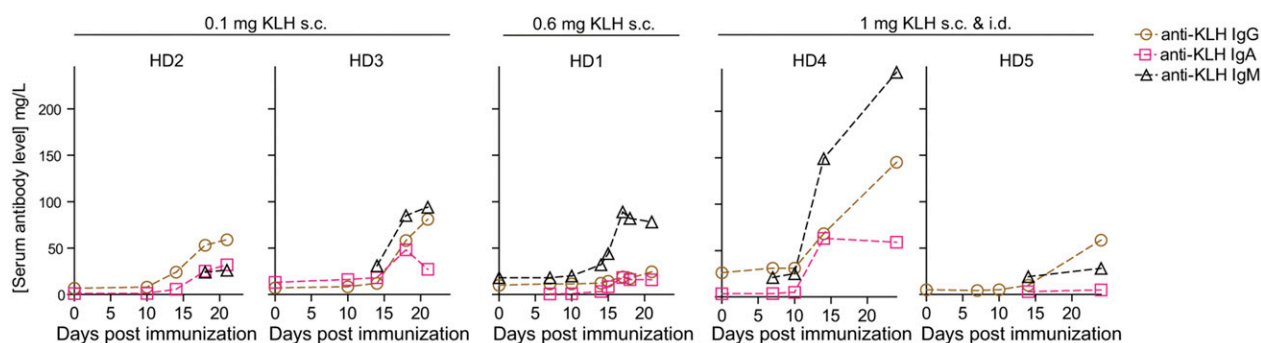
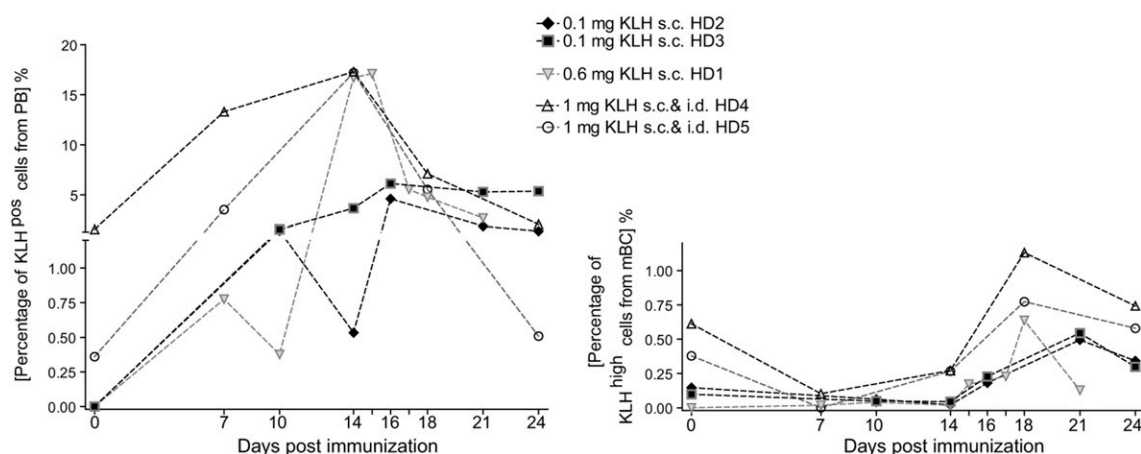
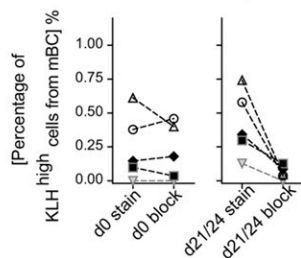
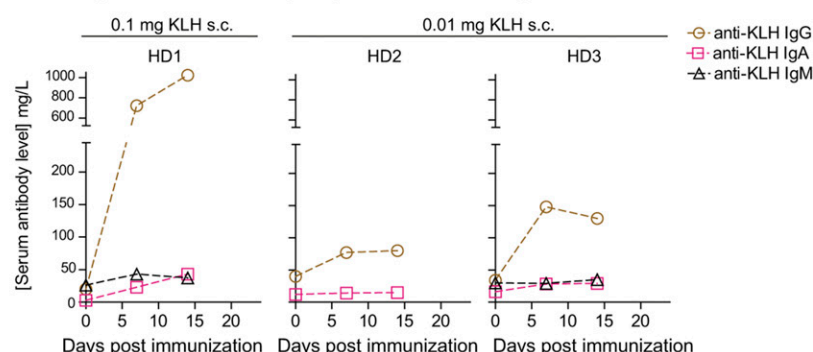
A KLH-specific serum antibody response after primary immunization**B** Peripheral blood KLH-specific plasmablast (left) and memory B cell (right) response**C** Block and stain of KLH-specific memory B cells**D** KLH-specific serum antibody response after secondary immunization

FIGURE 1. KLH-specific Ab and B cell kinetics in peripheral blood after primary and secondary parenteral KLH immunization. **(A)** Serum titers of KLH-specific IgA, IgM, and IgG Abs, respectively, after primary KLH immunization. No data point plotted means the sample was measured but the value was below the lower detection limit. **(B)** Kinetics of the frequency of peripheral blood KLH-specific plasmablasts analyzed by flow cytometry (left, gated as $CD3^+CD14^-CD19^+CD20^{low}CD27^{high}KLH^+$ cells) and KLH-specific mBCs (right, gated as $CD3^+CD14^-CD19^+CD20^+CD27^+KLH^{high}$ cells) at indicated time points after primary immunization expressed as percentages of the parent gate, respectively. Donors HD2 and HD3 received 0.1 mg KLH s.c., HD1 received 0.6 mg KLH s.c., and HD4 and HD5 received 1 mg KLH split into 0.5 mg s.c. and 0.5 mg i.d. in the upper arm. **(C)** Staining and blocking controls of KLH-specific mBCs before primary immunization and at the last sampled time point after primary immunization. Blocking controls were performed by adding unlabeled KLH in 50 \times excess to the PBMC prior to the staining with fluorochrome-labeled KLH. **(D)** Serum titers of KLH-specific IgA, IgM, and IgG Abs after secondary immunization, performed 6 mo (HD2 and HD3) or 18 mo (HD1), respectively, after primary immunization.

Abs, and establish lasting KLH-specific mBCs still detectable in the circulation, as known from other protein Ag vaccinations (21, 28).

Rapid induction of KLH-specific Abs and IgG dominance upon secondary KLH immunization

To evaluate the functional capacity of KLH-specific mBCs, we assessed the Ab response kinetics upon secondary KLH immunization

in the same three donors. In contrast to primary immunization, secondary Ab kinetics occurred faster, showed a higher magnitude and preferentially characterized by specific IgG. Anti-KLH IgG Ab titers showed a striking 2.0- to 36-fold increase and IgA Ab titers a 1.2- to 8-fold increase already on day 7 after reimmunization, whereas IgM Abs showed no noticeable change (Fig. 1D). These kinetics are reminiscent of recall responses (19) and thus consistent with the conclusion

that primary KLH immunization established a functional immune memory.

Primary circulating KLH-specific plasmablasts exhibit dominant IgA1 isotype usage

We also compared the isotype usage of the induced circulating KLH-specific plasmablasts after primary and secondary KLH immunization, respectively, as well as from steady-state KLH-specific mBCs. Therefore, we isolated individual cells at the respective time points (see Fig. 2A) by single-cell FACS followed by cDNA synthesis and nested PCR amplification of IgH V region—to-constant chain rearrangements. Between days 14 and 18 after primary KLH immunization, we recovered 207 functional sequences from circulating primary KLH-specific plasmablasts from all five donors. As shown in Fig. 2A, an overall predominance of IgA1 constant H chain (C α 1) usage was observed during all days (i.e., 42–90% of the sequences used the C α 1 chain) apart from HD2 on day 14. In three of the five donors, we found few KLH-specific plasmablasts using the C μ chain (26 from 207 sequences). Usage of IgG subclasses varied between donors and across various days, with frequent usage of the IgG constant H chain (C γ 1 and C γ 2 chain). The relative sequence isotype distribution of the circulating KLH-specific plasmablasts did not correlate with the corresponding serum IgG-to-IgA titer ratio. Precisely, KLH-specific serum IgG clearly dominated over IgA, which was not found for the IgG-to-IgA sequence ratio among circulating KLH-specific plasmablasts (Fig. 2B).

As described by our group and others before, secondary immunization induces a defined peak of circulating plasmablasts after 6–8 d (19). Accordingly, we detected and sorted individual KLH-specific plasmablasts for sequence analysis 7 d after secondary immunization. In this study, we could recover altogether 92 sequences. Notably, again, we found the C α 1 chain employed by a large proportion of the KLH-specific plasmablasts (38–53%) but a more frequent use of C γ chains. However, the ratio of the IgG-to-IgA isotype usage again did not correspond with the relative serum levels of anti-KLH IgG-to-IgA Abs (Fig. 2C).

IgH isotype usage of circulating KLH-specific mBCs shows only little overlap with KLH-specific plasmablasts

In HD1–HD3, we could analyze 36 IgH sequences from KLH-specific mBCs 2.5 mo after the primary immunization (i.e., 3.5 [HD2, HD3] to 15.5 mo [HD1] before secondary immunization). For HD1 and HD3, we found that the IgH isotype usage differed to that observed for KLH-specific primary and secondary plasmablasts. In general, there was a more pronounced C γ 1 and reduced C α 1 usage. Although the method is very sensitive to identify clones (21, 28), there is a possibility that the low clonal overlap could originate from the relatively low number of sequences found, a general limitation of Ag-specific mBC analyses.

Early appearance of highly mutated primary KLH-specific plasmablast sequences

To assess the characteristics of B cell diversification, the imprints of somatic hypermutation from V framework region (FWR) 1 through FWR3, allowing conclusions on their origin and differentiation history, were examined (Fig. 3A–C). Interestingly, 90% of the primary KLH-specific plasmablast sequences (187 out of 207) exhibited V gene mutations. The observed mutation frequencies of individual KLH-specific cells were not homogeneous between individual days and donors (Fig. 3A). Despite the lack of a characteristic stepwise increase of V gene mutations, highly mutated sequences among the circulating primary KLH-specific plasmablasts were present in all donors 2 wk after immunization. Specifically, 36% of the primary

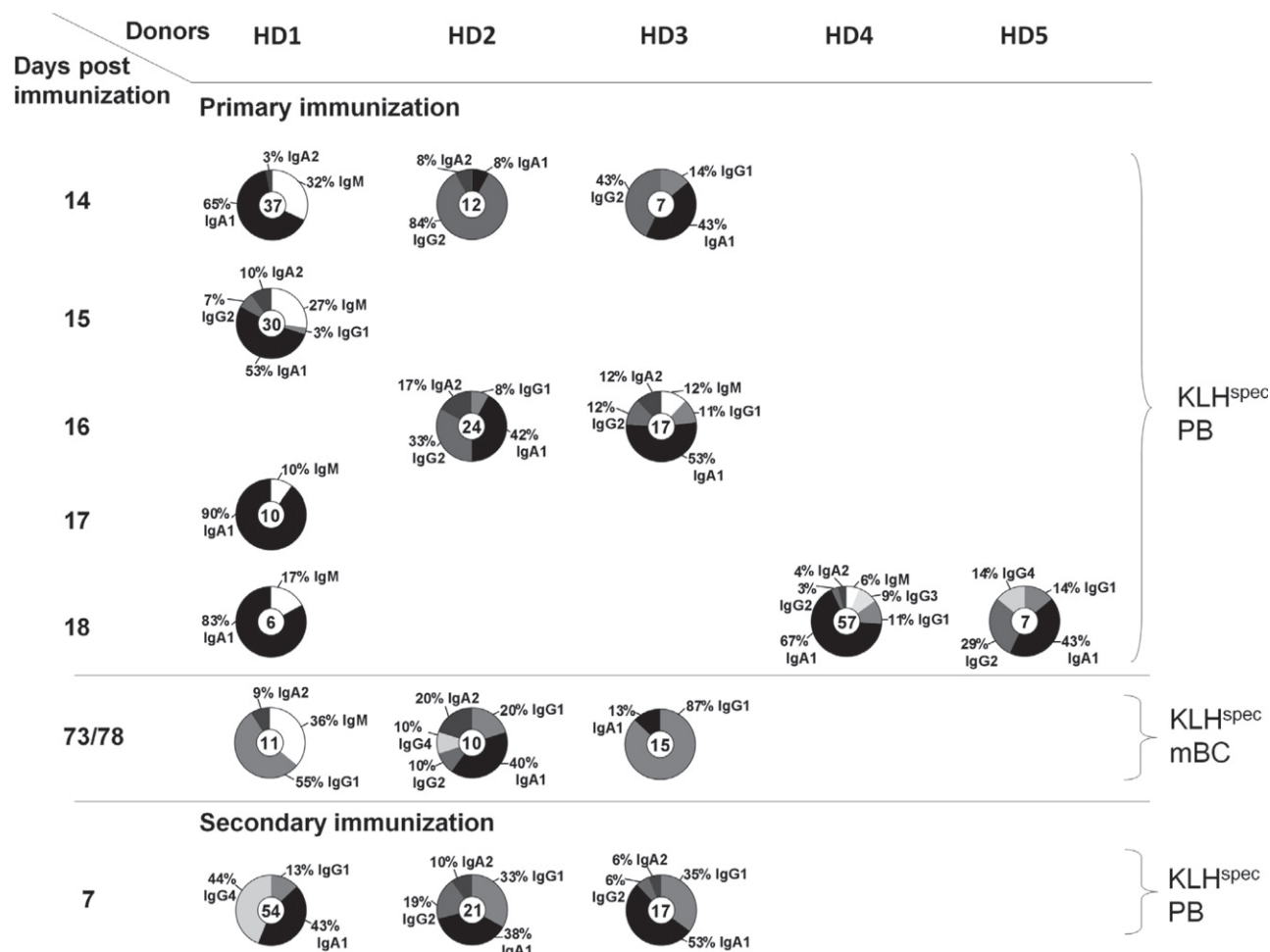
KLH-specific plasmablast sequences carried 15 mutations (Fig. 3B) or more (which translates into mutation frequencies $\geq 7\%$) within their IgH V rearrangements. Such high mutation frequencies have been reported for humoral memory responses, such as to annual influenza or to booster tetanus vaccination (21, 29, 30). It should be noted that there was no interrelation between highly mutated sequences and Ig isotype (Fig. 3C).

Theoretical considerations on the origin of highly mutated primary plasmablast sequences

We next asked whether primary plasmablasts characterized by highly mutated V genes could be generated from naive B cells within 2–3 wk as one of the possibilities to recruit de novo Ag-specific B cells. Some critical prerequisites for the acquisition of somatic hypermutations in B cell V genes have been discussed previously. Thus, it has been suggested that the somatic hypermutation machinery operates with a rate in a range of 4×10^{-4} to 1.1×10^{-3} mutations per bp per cell division (9, 10, 12, 31, 32) and that 7–18 h are required for B blast generation in GCs (8, 33). Accordingly, we calculated a theoretical mutation rate (mutation per bp per division) for each primary plasmablast sequence (Fig. 3D), as described before (10). We have taken a scenario into consideration assuming continuous division from the time point of KLH immunization to the respective day of blood drawing, with a fixed 8 h per cell cycle. This would translate into 42 cell cycles until day 14, 48 cycles until day 16, and 54 cycles until day 18. Under these circumstances, 43% of the primary KLH-specific plasmablast IgH sequences would have had mutation rates substantially higher than 1×10^{-3} mutations/bp per division (Fig. 3D). Moreover, on 8 out of the 10 sampling time points from all donors, the average mutation rate of the primary plasmablasts must have exceeded the predicted rate of 1×10^{-3} mutations/bp per generation (Fig. 3D). Vice versa, we have taken the mutation rate of 1×10^{-3} mutations/bp per generation as a precondition. Then, on average, 49% of these primary KLH-specific plasmablasts (day 14: 39%; day 16: 71%; and day 18: 40%) must have undergone continuous cell division with a <8-h cell cycle duration (data not shown). Additionally, we estimated the probability for the occurrence of at least a particular number of mutations for different mutation rates (Fig. 3E). As a result, with the previously described mutation rates, for clones found at day 14 with 25 mutations or more, the Poisson's probability of 10^{-5} would translate into the requirement of 10^5 naive precursor cells to be drawn into this response and to mutate to observe at least one cell with the particular mutation number (Fig. 3E). Extrapolating this required number of precursor cells that thus constitute one clonal family to the entire B cell repertoire, estimating the total number of lymphocytes in a human adult to be $\sim 460 \times 10^9$ (34), and assuming these would all be B cells, this would translate into a total B cell repertoire variety of 4.6×10^6 different clones. With respect to previous repertoire size estimates, this appears to be unlikely (1), apart from the fact that not all lymphocytes are B cells. For all calculations, it has to be emphasized that we did not consider any time window for GC onset or affinity selection or time for B cell differentiation followed by egress into the circulation, as we only had access to circulating cells. Truly, all these processes require time in addition that has to be subtracted from the calculated time frame GC B cells were given for cell division. Thus, the calculated values definitely must underestimate the actual mutation rates and rates of cell cycle durations naive B cells must have undergone, respectively, required to obtain the numbers of mutations observed. Therefore, we consider it unlikely that naive B cells were the precursors of these

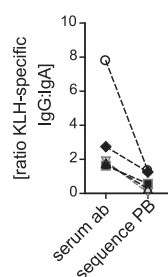
A

Isotype usage and distribution of KLH-specific IgH sequences



B

IgG to IgA ratio of KLH-specific serum antibodies and PB sequences after primary immunization



C

IgG to IgA ratio of KLH-specific serum antibodies and PB sequences after secondary immunization

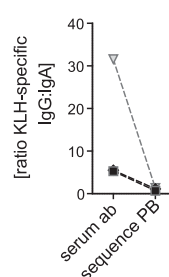


FIGURE 2. IgH sequence isotype usage of KLH-specific plasmablasts and mBCs. **(A)** Pie charts of the heavy constant chain isotype usage by KLH-specific plasmablasts (PB) and mBCs on indicated days after primary (HD1–HD5) and secondary immunization (HD1–HD3). Numbers in circles denote the number of productive sequences included. **(B)** Ratio of KLH-specific IgG-to-IgA levels from mean serum Ab levels (between days 14 and 24 after primary immunization) and IgH sequences (mean of respective isotype from total primary PB). **(C)** Ratio of KLH-specific IgG-to-IgA levels of serum Abs and KLH-specific PB sequences 7 d after secondary immunization.

highly mutated KLH-specific plasmablasts. This leads to the hypothesis that the highly mutated primary plasmablasts are the progeny of presumably cross-reactive mBCs recruited into the primary anti-KLH response.

Lack of global increase of V gene mutations from the primary to the secondary KLH-response

The amount of mutations can be used as a footprint of progress of affinity maturation of an immune response (12, 35, 36). With repeated

challenges, increasing amounts of somatic mutations within the V regions are expected. To investigate this aspect for the KLH response, we examined the changes of V gene mutations from the primary KLH-specific plasmablasts to the mBC and secondary plasmablast repertoire found in blood. In two of the three donors, circulating KLH-specific mBCs lacked highly mutated sequences, which were previously found in the primary plasmablast pool (Fig. 3A, Table I). It could be hypothesized either that mBC precursors left the GC response earlier than the plasmablast precursors, for which supporting

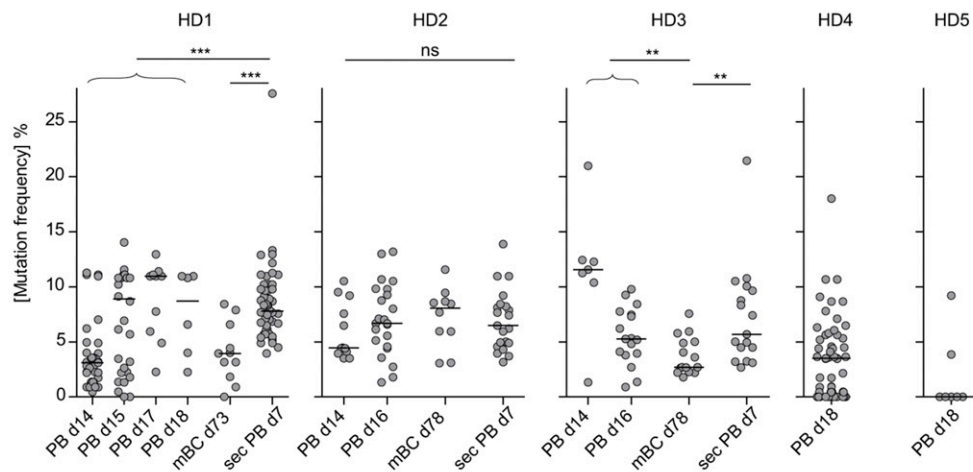
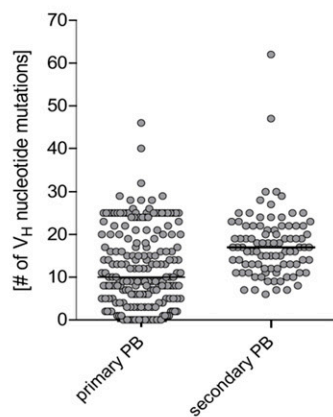
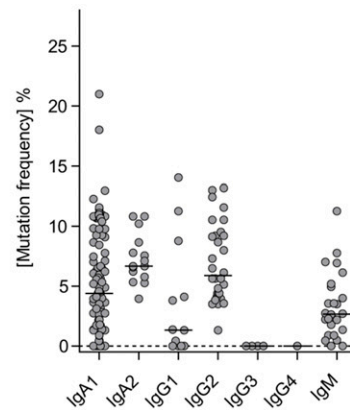
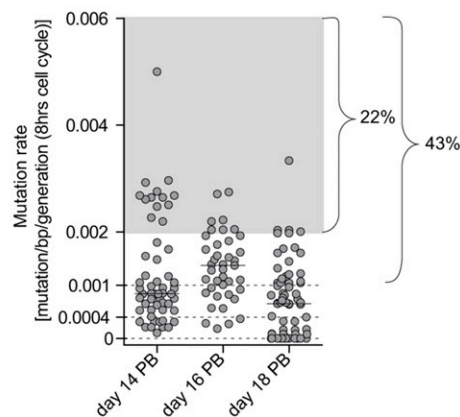
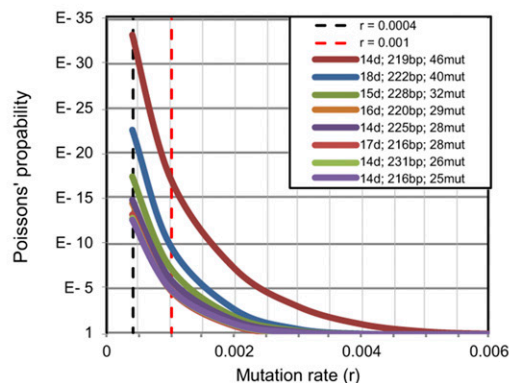
A Mutation frequency of KLH-specific primary plasmablasts (PB, d14-d18), mBC and secondary (sec) PB (d7)**B** Number of somatic mutations of primary and secondary PB**C** Mutation frequency to isotype of primary PB**D** Mutation rate of primary PB**E** Dependence of probability of number of mutations on mutation rate

FIGURE 3. Somatic hypermutation and theoretical estimation of mutation rates. **(A)** Frequencies of somatic hypermutation within IgH V regions (FWR1–FWR3) from individual KLH-specific plasmablasts or mBCs for each donor on indicated days. Each point represents the value for an individual IgH sequence. Mann–Whitney tests were performed with $p \leq 0.001$ represented by ***, $p \leq 0.01$ represented by **, and $p > 0.05$ considered as no significant difference (ns). For reasons of visual clarity, only significant differences revealed by testing are indicated for HD1 and HD3, whereas for HD2 no significant differences were found at all. **(B)** Number of somatic hypermutations in IgH V regions from KLH-specific primary and secondary plasmablasts. Data from individual donors were pooled. Bars indicate the median number of nucleotide substitutions. **(C)** Mutation frequencies of primary KLH-specific plasmablast sequences categorized according to their IgH isotype. Data from individual donors were pooled. **(D)** Calculated hypothetical mutation rates from individual KLH-specific primary plasmablasts determined from the number of accumulated mutations to the bp length of the V segment with an assumed cell cycle duration of 8 h. As reference, previously described mutation rates are indicated. Upper dotted line: 10^{-3} mutations/bp per generation (9); lower dotted line: 4×10^{-4} mutations/bp per generation (10). Brackets and frequencies indicate percentage of sequences that were theoretically subject to mutation rates higher than 1×10^{-3} (43%) or 2×10^{-3} (22%) mutations/bp per generation. **(E)** The probability for a particular number of mutations to occur at a particular mutation rate was estimated applying a Poisson distribution model. Plotted are the probabilities of the occurrence of at least the number of mutations (mut) for the eight least probable clones (found on indicated days) with an assumed division time of 8 h and different mutation rates. Red and black dotted lines again refer to the previously described mutation rates.

Table I. Summary of expressed IgH sequences of KLH-specific B cells

Donor	Day after Immunization	KLH-Specific B Cell Type	Sequences Mutated (%)	Mutations per V _H Median (Range)	R/S Ratio CDRH3-2	R/S Ratio FWR1-3	Total No. of Nucleotides	Total No. of Mutations	Median Mutation Rate ^a	No. of Sequences	No. of Unique Clones
HD1	14	PB	100	7 (1-25)	5.4	1.7	8,283	306	0.00074	37	18
HD1	15	PB	93	19.5 (0-32)	9	1.6	6,780	480	0.00198	30	19
HD1	17	PB	100	25 (5-28)	28.5	1.8	2,226	199	0.00215	10	5
HD1	18	PB	100	20 (5-25)	4	1.5	1,362	104	0.00161	6	4
HD1	73	mBC	91	9 (0-19)	4	1.3	2,469	100	n/a	11	11
HD1	7 ^b	PB	100	18 (9-62)	3.6	1.5	12,168	1027	n/a	54	49
HD2	14	PB	100	9 (8-24)	1.5	1.8	2,616	158	0.00106	12	5
HD2	16	PB	100	15 (3-29)	3.6	1.5	5,357	378	0.00139	24	12
HD2	78	mBC	100	16 (7-26)	4.8	2.1	2,181	158	n/a	10	9
HD2	7 ^b	PB	100	14 (7-30)	4.5	2	4,623	321	n/a	21	17
HD3	14	PB	100	26 (3-46)	3.9	1.7	1,578	180	0.00276	7	6
HD3	16	PB	100	12 (2-22)	4.8	1.5	3,819	210	0.00109	17	15
HD3	78	mBC	100	6 (4-17)	5.4	2.2	3,351	125	n/a	15	15
HD3	7 ^b	PB	100	13 (6-47)	4.7	1.7	3,756	273	n/a	17	14
HD4	18	PB	77	8 (0-40)	2.4	1.7	12,857	453	0.0006	57	32
HD5	18	PB	29	0 (0-21)	n/a ^c	n/a ^c	1,620	30	0	7	7

^aMutations per bp per generation (with 8-h cell cycle).^bDay after secondary immunization.^cNo S mutations were observed.n/a, not applicable; PB, plasmablast; V_H, V region H chain.

results from earlier experimental studies exist (37). Alternatively, as the repertoires were largely unrelated (described below), the progenitors of the highly mutated primary plasmablast sequences may not have been able to compete with the affinity increase of the originally less mutated cells. However, the general lack of clonal overlap as well as the lack of increased somatic hypermutations might be due to the low number of cells that could be sampled from peripheral blood, a known limiting factor for general conclusions on the repertoire.

After secondary immunization, all KLH-specific plasmablast sequences were found mutated. However, compared with primary KLH-specific plasmablasts, no significant increase of the median mutation frequency and number in HD2 and HD3 could be detected, whereas in HD1 the average increase of somatic mutations was significant (Mann-Whitney *U* test, $p < 0.001$; Fig. 3A). Yet for the latter, H chain complementarity-determining region 3 (CDRH3) length distribution showed a significant shift toward longer CDRH3s ($p < 0.01$, Mann-Whitney *U* test; Fig. 4A) and were more diverse compared with primary immunization CDRH3s. These findings suggest that the repertoires were rather different and therefore can, as such, not be used to demonstrate progressive mutation-dependent affinity maturation of the initial clonal lineages detected after primary immunization.

CDRH3 length distributions are characteristic of a restricted repertoire

We next analyzed the CDRH3 length distribution in more detail, as the CDRH3 is a major determinant of Ag binding, and an Ag-selected repertoire should show restrictions in its CDRH3 usage and average length. We found a restricted distribution of the CDRH3 lengths of KLH-specific plasmablasts and mBCs, indicating oligoclonal to limited polyclonal repertoires (Fig. 4A). The narrow CDRH3 length distribution compared with naive B cell repertoires (38, 39) together with the preference for CDRH replacement (R) over silent (S) mutations in contrast to FWRs suggests that the immunization-induced KLH-specific B cells were functionally selected (i.e., GC-derived) (Table I).

Minor between-day repertoire changes in the circulating primary KLH-specific plasmablast pool

Having identified the restricted CDRH3 length distribution, we next analyzed the KLH-specific B cell clonal composition. We defined a clone by its unique IgH V region sequence, including the CDRH3 length and sequence. Sequences belonging to a clone (i.e., clonal lineage) should have the very same sequence yet allow for shared as well as unique mutations, as described before (21). This analysis identified several expanded clonal relationships within KLH-specific B cells of HD1-HD4, but no sequence qualifying as clonally related was found between individual donors. Pies of the circulating KLH-specific plasmablast and mBC repertoires are shown in Fig. 4B.

Primary plasmablast repertoires showed some variations between different sample days (pies HD1-HD3). To further estimate the extent of repertoire fluctuations, a statistical analysis of the theoretical repertoire sizes was performed as described (21, 25). This calculation yielded relatively small KLH-specific primary plasmablast repertoires, supporting the assumption that these plasmablasts were Ag selected. Furthermore, this calculation further illustrated variation of daily repertoire sizes and supported the notion that the circulating primary plasmablasts were undergoing turnover between the sampled days. Overall, the data imply that plasmablasts gradually left secondary lymphoid tissues to migrate via the blood stream to a potential survival niche as suggested before (i.e., the bone marrow) (40-43) (Fig. 4B).

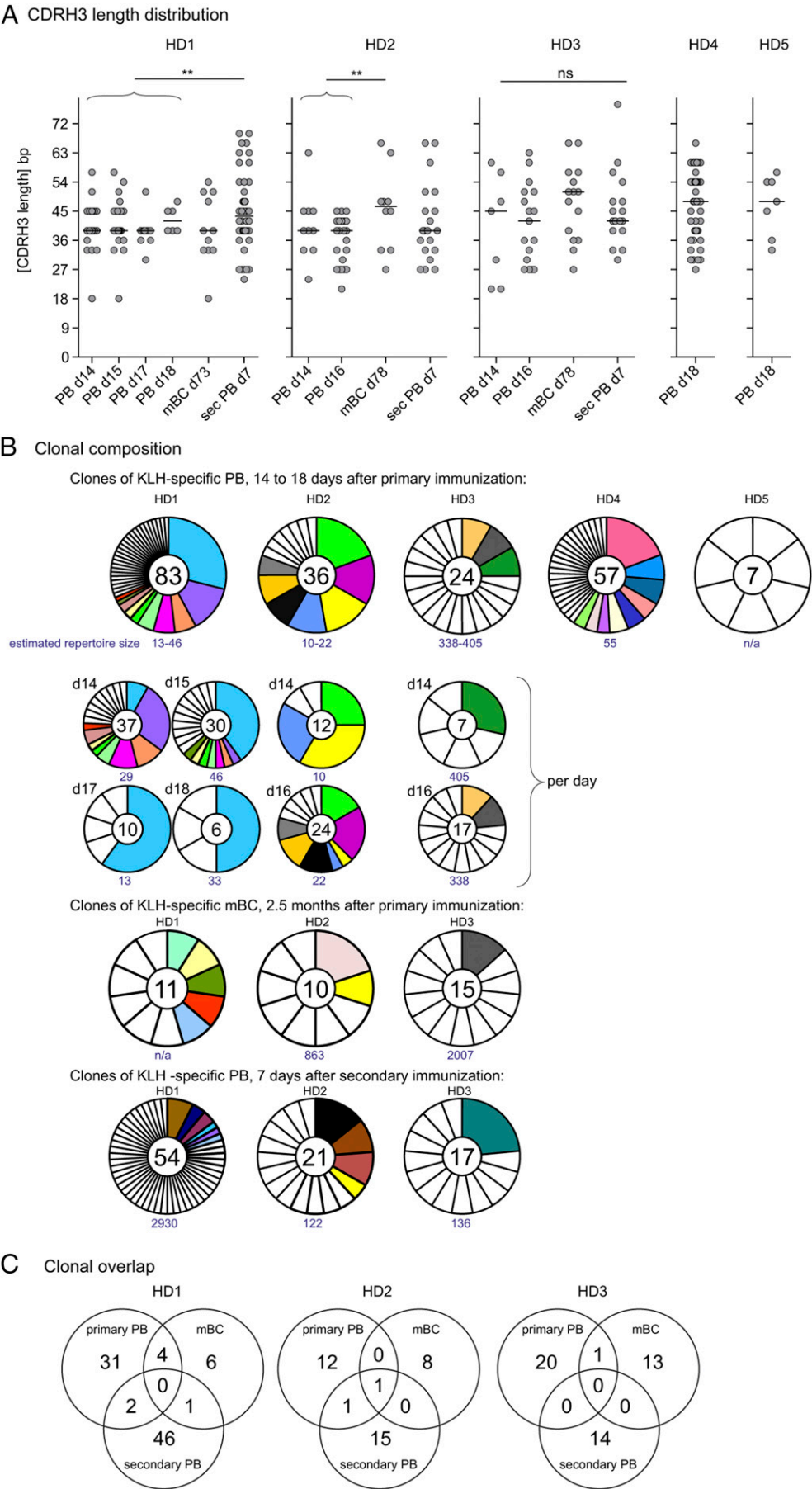


FIGURE 4. KLH-specific B cell CDRH3 lengths and repertoires. **(A)** Distribution of CDRH3 lengths in bp of KLH-specific plasmablasts and mBCs for each donor and day as indicated. Bar indicates median values. Mann-Whitney tests were performed, with $p \leq 0.01$ (Figure legend continues)

Circulating KLH-specific primary, memory, and secondary B cell pools carry distinct BCR gene repertoires

To identify clonal overlaps and preferred selection of specific clones, we finally analyzed the clonal composition of KLH-specific primary plasmablasts, mBCs, and secondary plasmablasts. Analysis of KLH-specific mBCs from HD2 identified one mBC clone (yellow slice) for which clonally related primary plasmablasts were found (Fig. 4B, 4C). Similarly, for HD3, one mBC clone was found that was clonally related to a primary plasmablast clone. For HD1, four KLH-specific mBC clones were found for which clonally related primary plasmablasts were identified.

Strikingly, secondary KLH-specific plasmablasts comprised a largely distinct repertoire compared with the primary KLH-specific plasmablasts. Although we could retrieve in total four clones from the secondary plasmablast sequences that belonged to KLH-specific clones already present in the primary KLH-specific plasmablast repertoire (Fig. 4B, 4C), the majority of secondary plasmablast sequences were neither related to the primary plasmablast repertoire nor to the circulating mBCs 2.5 mo after primary immunization. Moreover, theoretical repertoire size calculations yielded for HD1 and HD2 clonally more diverse secondary KLH-specific plasmablast repertoires (Fig. 4B). Taken together, albeit with limitations, analysis of the clonal relationships detected largely different KLH-specific B cell repertoires between circulating primary plasmablasts, steady-state mBCs, and secondary plasmablasts.

Discussion

Human B cell responses are predominantly studied either after convalescence or after an indefinite time point upon infection by measuring Ab titers. Only some studies reported detailed data on Ag-specific B cells upon booster immunization (some summarized in Ref. 44); however, the number of previous exposure(s) varied substantially. In this study, we analyzed the Ag-specific serological Ig response together with the IgH V sequence repertoire of Ag-specific plasmablasts and mBCs in the course of parenteral primary and secondary KLH immunization in human adults. This permitted direct comparison of the characteristics of a defined naive and mBC response.

Although Ab kinetics between the primary and secondary immunization followed described patterns, the simultaneous appearance of primary IgM, IgA, and IgG Abs; the robust appearance of anti-KLH IgA Abs; the high somatic mutation frequencies in one third of primary plasmablasts; and the minimal clonal overlap between primary and secondary responses was unexpected but provides new insights into human parenteral immune responses.

First, a robust Ag-specific IgA induction, as reported by other studies using parenteral T cell-dependent challenges (18, 45, 46), was observed against KLH and suggests an underappreciated importance of serum IgA for systemic immune protection. Moreover, complementary to serum IgA, we detected also KLH-specific IgA expressing plasmablasts and mBCs. Although one study (46) reported that IgA expressing B cell subsets contracted

after repeated parenteral T cell-dependent immunization, another study investigating age-related changes in human peripheral blood IgH repertoires found that there was a striking age-related correlation between protection and the IgA response (47). The current study further found a discrepancy between the KLH-specific serum IgG-to-IgA ratio and the ratio of obtained IgG-to-IgA isotypes of KLH-specific plasmablasts isolated from peripheral blood, consistent with recent data by Wimmers et al. (46). The pronounced peripheral blood KLH-specific IgA plasmablast wave observed in this and other studies (46) upon parenteral immunization indicates possible distinct functions, and there might be a distinct role of serum IgA versus IgG in systemic protection (47). Alternatively, these cellular subsets might underlie different regulations, as has been suggested for tetanus-specific mBCs and plasma cells (48). In this regard, one study showed that the relative contribution of vaccination-induced peripheral blood plasmablasts to serological immunity appears to be rather low because the corresponding repertoires did not correlate well (30).

Repertoire analyses revealed a sparse clonal overlap between KLH-specific primary plasmablasts, mBCs, and secondary plasmablast repertoires. The mere presence of even few clonally related primary and secondary plasmablast sequences can be taken as genetic evidence of established and reactivated B cell memory. Interestingly, the secondary plasmablast pool appeared clonally more diverse than the primary effector B cell pool. A response-to-response variation regarding the participation of individual clonotypes together with a loss of dominating primary clones in the memory repertoire has been termed repertoire shift (10, 14, 15, 49, 50). Although our study has its admitted limitations due to the low number of sequences, this repertoire shift and the lack of a clear increase of somatic hypermutations in the KLH-specific secondary plasmablasts could suggest that clonal selection continued after termination of the primary GC response [including active somatic hypermutation after 2–3 wk (8)]. This suggestion would be consistent with observations in experimental models (51, 52). Recent studies also demonstrated elegantly that the majority of bone marrow plasma cells are generated after the peak GC response and continue for at least 1 mo, whereas the process of somatic hypermutation appeared to be discontinued after ~2 wk (37). Our sampling period ended 3 wk after vaccination, a time point when few circulating KLH-specific plasmablasts were still detectable. Future studies should therefore expand the time frame of such a longitudinal analysis.

One could hypothesize that late or post-GC selection may result in a distinct interclonal competition compared with the early phase. Such a concept would allow continuing improvement of the Ag-selected repertoire while keeping the repertoire broad enough to react toward pathogen variants without mutation-driven convergence toward one specific high-affinity clone. The latter would bear the risk of its deletion by introducing deleterious mutations. Alternatively, the repertoire shift could also occur only upon reactivation, when there are still enough Abs present to cover major epitopes for which primary effector B cells competed. In such a scenario, hitherto unrecognized epitopes could react with

represented by ** and $p > 0.05$ considered as no significant difference (ns). For reasons of visual clarity, only the significant differences revealed by testing are indicated for HD1 and HD2, whereas for HD3 no significant differences were found at all. (B) Pie charts represent different clonal families of KLH-specific plasmablasts and mBCs. Primary plasmablasts for each donor are shown for days 14–18 (pooled and per day where applicable). Circled number within each pie chart denotes the total number of sequences; slices are unique clones and proportional to clone size. KLH-specific plasmablast sequences that were found only once between days 14 and 18, for which clonally related cells were found in the KLH-specific mBC or secondary plasmablast compartment, were also marked by a color piece. White slices denote those sequences found only once during the entire response. Numbers underneath the pies are the one-sided 95% confidence limits of the maximum likelihood estimates of the repertoire sizes, calculated as described before (21, 25). (C) Venn diagrams show clonal overlap of KLH-specific primary plasmablasts (PB), mBC, and secondary PB sequences for HD1–HD3. The total number of unique clones in the respective compartment is indicated.

cross-reactive mBCs for which memory T cell help should then, however, be present, resulting in a memory response kinetic. The induced specific plasmablast repertoire would then largely differ to the primary response plasmablast pool. It is conceivable that this scenario repeats several times until all available epitopes are recognized by serum Abs. In support of this idea is the observation that long time periods and repeated rounds of (sequentially evolving variants of) antigenic stimulation are required to generate highly mutated cells, as observed in HIV patients and elegant preclinical models (53).

Another intriguing finding of our study is the detection of highly mutated IgH sequences within the primary KLH-specific plasmablast pool, of which the mutated sequences clearly showed signs of functional selection. Highly mutated sequences early during a primary response were recently also described by Galson et al. (54). Based on our calculations, naive B cells carrying unmutated IgH sequences are unlikely to obtain such a high mutation frequency within 14–18 d after primary activation (Fig. 3D, 3E). Therefore, we propose that highly mutated primary plasmablasts that were selected by KLH binding represent descendants of mBCs with a cross-reactive specificity. Whereas higher mutation frequencies have been described to correlate with higher affinities (55, 56), providing increased survival fitness, we found the simultaneous presence of nonmutated and highly mutated KLH-specific plasmablasts early during the response without dominant expansion of highly mutated cells. Yet, only re-expression and affinity testing of the high- and low-mutated KLH-specific Ig sequences could provide evidence to support or reject this hypothesis, which is the subject of future studies.

The hypothesized activation of cross-specific mBCs did not result in kinetics characteristic of memory responses (19, 57) but rather those of primary Ag contact (18, 57). We hypothesize that cognate KLH-specific memory T cells are lacking, and thus the fast generation of plasmablasts is compromised. In support of this notion are observations of primary responses in primed versus unprimed rat model systems; in the former case, pre-existing T cell help caused faster appearance of specific B cells (8). However, because other studies have suggested that mBCs do not rely on T cell help for their reactivation (58–60), the role of T cell help in mBC reactivation remains uncertain and may depend on the system analyzed. Notably, however, experiments by Weisel et al. (61) showed that homing of mBCs to lymphoid follicle structures was required for their reactivation, indicating that mBCs' BCR binding to an Ag is not sufficient for their reactivation, and accessory help provided in secondary lymphoid organs seems to be required. Our observations of KLH-binding mBCs prior to primary KLH immunization, their disappearance shortly afterward, and subsequent reappearance suggest the possibility of their tissue-dependent maturation including temporary lymphoid tissue retention, as reported by others (61, 62).

Cross-reactivity of the mBC pool may be of relevance also in autoimmunity. As every large protein can be bound by a specific BCR, it is conceivable that cognate BCR from mBCs are not excluded (as long as certain costimulatory signals are available) regardless of whether this Ag is a new or an anamnestic one. Moreover, because the mBC population comprises 30–40% of the B cell pool in human adults (28), it appears uneconomical for the immune system to specifically exclude mBCs from primary responses. However, potentially self-antigen specific mBCs have to be tightly controlled to avoid autoreactivity, and the mechanism(s) involved remain to be elucidated.

In conclusion, based on the known complexity of the human B cell Ig V germline repertoire, the Ab response to a stimulus becomes less predictable as the immune history of an individual

considerably shapes the serologic and cellular repertoire (63). This has consequences for future vaccine design and potential immunization schedules of follow-up vaccines if the aim is to generate a convergent (broadly neutralizing) Ab response as currently discussed (53). The results from a recent study investigating the B cell response to Zika virus infection in dengue virus-experienced individuals (63) further support these notions. This study found that the conserved regions between both flaviviruses caused cross-reactive mBC reactivation with a massive plasmablast expansion 8 d upon symptom onset, consistent with the response-accelerating effect of pre-existing T cell help in a primed system discussed above. Notably, this cross-reactive memory was poorly neutralizing, although it carried binding capacity, a phenomenon already described for HIV gp41-specific mBCs (64, 65). The study by Rogers et al. also tested a Dengue virus-naïve donor infected with Zika. This donor lacked an early massive plasmablast response and the nonneutralizing cross-reactivity with Dengue virus. Instead, this donor's Abs showed largely, albeit weak, neutralizing activity, pointing toward the importance of understanding cross-reactivity and its effects on immune and vaccination responses. In accordance with our data, albeit in a different system, the study demonstrated the lack of clonal overlap of Zika virus primary (day 8) plasmablasts and specific mBCs recovered 5 mo thereafter. Furthermore, in the primary response repertoire of the naive donor, they detected largely unmutated primary plasmablasts but also found a few highly mutated clones, again consistent with our results.

Acknowledgments

We thank J. Kirsch and T. Kaiser for excellent assistance with cell sorting and T. Geske, H. Hecker-Kia, H. Schliemann, A. Peddinghaus, K. Reiter, M. Sackl, and U. Dethlefs for excellent technical assistance. We thank C. Berek, A. Hutloff, and U. Klein for critical discussions and interpretation of the data.

Disclosures

The authors have no financial conflicts of interest.

References

- Glanville, J., W. Zhai, J. Berka, D. Telman, G. Huerta, G. R. Mehta, I. Ni, L. Mei, P. D. Sundar, G. M. Day, et al. 2009. Precise determination of the diversity of a combinatorial antibody library gives insight into the human immunoglobulin repertoire. *Proc. Natl. Acad. Sci. USA* 106: 20216–20221.
- Steiner, L. A., and H. N. Eisen. 1967. Sequential changes in the relative affinity of antibodies synthesized during the immune response. *J. Exp. Med.* 126: 1161–1183.
- Eisen, H. N., and G. W. Siskind. 1964. Variations in affinities of antibodies during the immune response. *Biochemistry* 3: 996–1008.
- Zotos, D., and D. M. Tarlinton. 2012. Determining germinal centre B cell fate. *Trends Immunol.* 33: 281–288.
- MacLennan, I. C., K. M. Toellner, A. F. Cunningham, K. Serre, D. M. Sze, E. Zúñiga, M. C. Cook, and C. G. Vinuesa. 2003. Extrafollicular antibody responses. *Immunol. Rev.* 194: 8–18.
- Shlomchik, M. J., and F. Weisel. 2012. Germinal centers. *Immunol. Rev.* 247: 5–10.
- Jacob, J., G. Kelsoe, K. Rajewsky, and U. Weiss. 1991. Intracлонаl generation of antibody mutants in germinal centres. *Nature* 354: 389–392.
- Liu, Y. J., J. Zhang, P. J. Lane, E. Y. Chan, and I. C. MacLennan. 1991. Sites of specific B cell activation in primary and secondary responses to T cell-dependent and T cell-independent antigens. *Eur. J. Immunol.* 21: 2951–2962.
- McKean, D., K. Huppi, M. Bell, L. Staudt, W. Gerhard, and M. Weigert. 1984. Generation of antibody diversity in the immune response of BALB/c mice to influenza virus hemagglutinin. *Proc. Natl. Acad. Sci. USA* 81: 3180–3184.
- Berek, C., and C. Milstein. 1987. Mutation drift and repertoire shift in the maturation of the immune response. *Immunol. Rev.* 96: 23–41.
- Neuberger, M. S., and C. Milstein. 1995. Somatic hypermutation. *Curr. Opin. Immunol.* 7: 248–254.
- Sablitzky, F., G. Wildner, and K. Rajewsky. 1985. Somatic mutation and clonal expansion of B cells in an antigen-driven immune response. *EMBO J.* 4: 345–350.
- Allen, D., A. Cumano, R. Dildrop, C. Kocks, K. Rajewsky, N. Rajewsky, J. Roes, F. Sablitzky, and M. Siekevitz. 1987. Timing, genetic requirements and functional

- consequences of somatic hypermutation during B-cell development. *Immunol. Rev.* 96: 5–22.
14. Berek, C., J. M. Jarvis, and C. Milstein. 1987. Activation of memory and virgin B cell clones in hyperimmune animals. *Eur. J. Immunol.* 17: 1121–1129.
 15. Reth, M., G. J. Hämmerling, and K. Rajewsky. 1978. Analysis of the repertoire of anti-NP antibodies in C57BL/6 mice by cell fusion. I. Characterization of antibody families in the primary and hyperimmune response. *Eur. J. Immunol.* 8: 393–400.
 16. Harris, J. R., and J. Markl. 1999. Keyhole limpet hemocyanin (KLH): a biomedical review. *Micron* 30: 597–623.
 17. Burke, G. P., K. A. Smith, R. I. Stocking, M. Ferm, and O. R. McIntyre. 1977. Anti-keyhole limpet hemocyanin antibody in normal unsensitized individuals. *J. Allergy Clin. Immunol.* 59: 309–313.
 18. Blanchard-Rohner, G., A. S. Pulickal, C. M. Jol-van der Zijde, M. D. Snape, and A. J. Pollard. 2009. Appearance of peripheral blood plasma cells and memory B cells in a primary and secondary immune response in humans. *Blood* 114: 4998–5002.
 19. Fink, K. 2012. Origin and function of circulating plasmablasts during acute viral infections. *Front. Immunol.* 3: 78.
 20. Aarntzen, E. H., I. J. de Vries, J. H. Göertz, M. Beldhuis-Valkis, H. M. Brouwers, M. W. van de Rakt, R. G. van der Molen, C. J. Punt, G. J. Adema, P. J. Tacken, et al. 2012. Humoral anti-KLH responses in cancer patients treated with dendritic cell-based immunotherapy are dictated by different vaccination parameters. *Cancer Immunol. Immunother.* 61: 2003–2011.
 21. Frölich, D., C. Giesecke, H. E. Mei, K. Reiter, C. Daridon, P. E. Lipsky, and T. Dörner. 2010. Secondary immunization generates clonally related antigen-specific plasma cells and memory B cells. *J. Immunol.* 185: 3103–3110.
 22. Campbell, M. J., A. D. Zelenetz, S. Levy, and R. Levy. 1992. Use of family specific leader region primers for PCR amplification of the human heavy chain variable region gene repertoire. *Mol. Immunol.* 29: 193–203.
 23. Marks, J. D., M. Tristram, A. Karpas, and G. Winter. 1991. Oligonucleotide primers for polymerase chain reaction amplification of human immunoglobulin variable genes and design of family-specific oligonucleotide probes. *Eur. J. Immunol.* 21: 985–991.
 24. Souto-Carneiro, M. M., N. S. Longo, D. E. Russ, H. W. Sun, and P. E. Lipsky. 2004. Characterization of the human Ig heavy chain antigen binding complementarity determining region 3 using a newly developed software algorithm, JOINSOLVER. *J. Immunol.* 172: 6790–6802.
 25. Behlke, M. A., D. G. Spinella, H. S. Chou, W. Sha, D. L. Hartl, and D. Y. Loh. 1985. T-cell receptor beta-chain expression: dependence on relatively few variable region genes. *Science* 229: 566–570.
 26. Sprent, J., J. F. Miller, and G. F. Mitchell. 1971. Antigen-induced selective recruitment of circulating lymphocytes. *Cell. Immunol.* 2: 171–181.
 27. Kohler, S., N. Bethke, M. Böthe, S. Sommerick, M. Frentsch, C. Romagnani, M. Niedrig, and A. Thiel. 2012. The early cellular signatures of protective immunity induced by live viral vaccination. *Eur. J. Immunol.* 42: 2363–2373.
 28. Giesecke, C., D. Frölich, K. Reiter, H. E. Mei, I. Wirries, R. Kuhly, M. Killig, T. Glatzer, K. Stölzel, C. Perka, et al. 2014. Tissue distribution and dependence of responsiveness of human antigen-specific memory B cells. *J. Immunol.* 192: 3091–3100.
 29. Wrämmert, J., K. Smith, J. Miller, W. A. Langley, K. Kokko, C. Larsen, N. Y. Zheng, I. Mays, L. Garman, C. Helms, et al. 2008. Rapid cloning of high-affinity human monoclonal antibodies against influenza virus. *Nature* 453: 667–671.
 30. Lavinder, J. J., Y. Wine, C. Giesecke, G. C. Ippolito, A. P. Horton, O. I. Lungu, K. H. Hoi, B. J. DeKosky, E. M. Murrin, M. M. Wirth, et al. 2014. Identification and characterization of the constituent human serum antibodies elicited by vaccination. *Proc. Natl. Acad. Sci. USA* 111: 2259–2264.
 31. Levy, N. S., U. V. Malipiero, S. G. Lebecque, and P. J. Gearhart. 1989. Early onset of somatic mutation in immunoglobulin VH genes during the primary immune response. *J. Exp. Med.* 169: 2007–2019.
 32. Kleinstein, S. H., Y. Louzoun, and M. J. Shlomchik. 2003. Estimating hypermutation rates from clonal tree data. *J. Immunol.* 171: 4639–4649.
 33. Zhang, J., I. C. MacLennan, Y. J. Liu, and P. J. Lane. 1988. Is rapid proliferation in B centroblasts linked to somatic mutation in memory B cell clones? *Immunol. Lett.* 18: 297–299.
 34. Trepel, F. 1974. Number and distribution of lymphocytes in man. A critical analysis. *Klin. Wochenschr.* 52: 511–515.
 35. Rajewsky, K., I. Förster, and A. Cumano. 1987. Evolutionary and somatic selection of the antibody repertoire in the mouse. *Science* 238: 1088–1094.
 36. Eisen, H. N. 2014. Affinity enhancement of antibodies: how low-affinity antibodies produced early in immune responses are followed by high-affinity antibodies later and in memory B-cell responses. *Cancer Immunol. Res.* 2: 381–392.
 37. Weisel, F. J., G. V. Zuccarino-Catania, M. Chikina, and M. J. Shlomchik. 2016. A temporal switch in the germinal center determines differential output of memory B and plasma cells. *Immunity* 44: 116–130.
 38. Elhanati, Y., Z. Sethna, Q. Marcou, C. G. Callan, Jr., T. Mora, and A. M. Walczak. 2015. Inferring processes underlying B-cell repertoire diversity. *Philos. Trans. R. Soc. Lond. B Biol. Sci.* DOI: 10.1098/rstb.2014.0243.
 39. DeWitt, W. S., P. Lindau, T. M. Snyder, A. M. Sherwood, M. Vignali, C. S. Carlson, P. D. Greenberg, N. Duerkopp, R. O. Emerson, and H. S. Robins. 2016. A public database of memory and naive B-cell receptor sequences. *PLoS One* 11: e0160853.
 40. Mei, H. E., I. Wirries, D. Frölich, M. Brissler, C. Giesecke, J. R. Grün, T. Alexander, S. Schmidt, K. Luda, A. A. Kühl, et al. 2015. A unique population of IgG-expressing plasma cells lacking CD19 is enriched in human bone marrow. *Blood* 125: 1739–1748.
 41. Odendahl, M., H. Mei, B. F. Hoyer, A. M. Jacobi, A. Hansen, G. Muehlinghaus, C. Berek, F. Hiepe, R. Manz, A. Radbruch, and T. Dörner. 2005. Generation of migratory antigen-specific plasma blasts and mobilization of resident plasma cells in a secondary immune response. *Blood* 105: 1614–1621.
 42. Medina, F., C. Segundo, A. Campos-Caro, I. González-García, and J. A. Brieva. 2002. The heterogeneity shown by human plasma cells from tonsil, blood, and bone marrow reveals graded stages of increasing maturity, but local profiles of adhesion molecule expression. *Blood* 99: 2154–2161.
 43. Blink, E. J., A. Light, A. Kallies, S. L. Nutt, P. D. Hodgkin, and D. M. Tarlinton. 2005. Early appearance of germinal center-derived memory B cells and plasma cells in blood after primary immunization. *J. Exp. Med.* 201: 545–554.
 44. Trück, J., M. N. Ramasamy, J. D. Galson, R. Rance, J. Parkhill, G. Lunter, A. J. Pollard, and D. F. Kelly. 2015. Identification of antigen-specific B cell receptor sequences using public repertoire analysis. *J. Immunol.* 194: 252–261.
 45. Mascart-Lemone, F., J. Duchateau, M. E. Conley, and D. L. Delacroix. 1987. A polymeric IgA response in serum can be produced by parenteral immunization. *Immunology* 61: 409–413.
 46. Wimmers, F., N. de Haas, A. Scholzen, G. Schreibelt, E. Simonetti, M. J. Eleveld, H. M. Brouwers, M. Beldhuis-Valkis, I. Joosten, M. I. de Jonge, et al. 2017. Monitoring of dynamic changes in keyhole limpet hemocyanin (KLH)-specific B cells in KLH-vaccinated cancer patients. *Sci. Rep.* 7: 43486.
 47. Wu, Y. C., D. Kipling, and D. K. Dunn-Walters. 2012. Age-related changes in human peripheral blood IGH repertoire following vaccination. *Front. Immunol.* 3: 193.
 48. Leyendeckers, H., M. Odendahl, A. Löhndorf, J. Irsch, M. Spangfort, S. Miltenyi, N. Hunzelmann, M. Assenmacher, A. Radbruch, and J. Schmitz. 1999. Correlation analysis between frequencies of circulating antigen-specific IgG-bearing memory B cells and serum titers of antigen-specific IgG. *Eur. J. Immunol.* 29: 1406–1417.
 49. Kavalier, J., A. J. Caton, L. M. Staudt, and W. Gerhard. 1991. A B cell population that dominates the primary response to influenza virus hemagglutinin does not participate in the memory response. *Eur. J. Immunol.* 21: 2687–2695.
 50. Stenzel-Poore, M. P., U. Bruderer, and M. B. Rittenberg. 1988. The adaptive potential of the memory response: clonal recruitment and epitope recognition. *Immunol. Rev.* 105: 113–136.
 51. Davie, J. M., and W. E. Paul. 1972. Receptors on immunocompetent cells. V. Cellular correlates of the “maturation” of the immune response. *J. Exp. Med.* 135: 660–674.
 52. Takahashi, Y., P. R. Dutta, D. M. Cerasoli, and G. Kelsoe. 1998. In situ studies of the primary immune response to (4-hydroxy-3-nitrophenyl)acetyl. V. Affinity maturation develops in two stages of clonal selection. *J. Exp. Med.* 187: 885–895.
 53. Escolano, A., J. M. Steichen, P. Dosenovic, D. W. Kulp, J. Golijanin, D. Sok, N. T. Freund, A. D. Gitlin, T. Oliveira, T. Araki, et al. 2016. Sequential immunization elicits broadly neutralizing anti-HIV-1 antibodies in Ig knockin mice. *Cell* 166: 1445–1458.e1412.
 54. Galson, J. D., J. Trück, E. A. Clutterbuck, A. Fowler, V. Cerundolo, A. J. Pollard, G. Lunter, and D. F. Kelly. 2016. B-cell repertoire dynamics after sequential hepatitis B vaccination and evidence for cross-reactive B-cell activation. [Published erratum appears in 2016 *Genome Med.* 8: 81.] *Genome Med.* 8: 68.
 55. Smith, K. G., A. Light, G. J. Nossal, and D. M. Tarlinton. 1997. The extent of affinity maturation differs between the memory and antibody-forming cell compartments in the primary immune response. *EMBO J.* 16: 2996–3006.
 56. Pappas, L., M. Foglierini, L. Piccoli, N. L. Kallewaard, F. Turrini, C. Silacci, B. Fernandez-Rodriguez, G. Agatic, I. Giacchetto-Sasselli, G. Pellicciotta, et al. 2014. Rapid development of broadly influenza neutralizing antibodies through redundant mutations. *Nature* 516: 418–422.
 57. Heffner, R. R., Jr., and A. Schluederberg. 1967. Specificity of the primary and secondary antibody responses to myxoviruses. *J. Immunol.* 98: 668–672.
 58. Zuccarino-Catania, G. V., S. Sadanand, F. J. Weisel, M. M. Tomayko, H. Meng, S. H. Kleinstein, K. L. Good-Jacobson, and M. J. Shlomchik. 2014. CD80 and PD-L2 define functionally distinct memory B cell subsets that are independent of antibody isotype. *Nat. Immunol.* 15: 631–637.
 59. Hebeis, B. J., K. Klenovsek, P. Rohwer, U. Ritter, A. Schneider, M. Mach, and T. H. Winkler. 2004. Activation of virus-specific memory B cells in the absence of T cell help. *J. Exp. Med.* 199: 593–602.
 60. Klinman, N. R., and R. A. Doughty. 1973. Hapten-specific stimulation of secondary B cells independent of T cells. *J. Exp. Med.* 138: 473–478.
 61. Weisel, F. J., U. K. Appelt, A. M. Schneider, J. U. Horlitz, N. van Rooijen, H. Korner, M. Mach, and T. H. Winkler. 2010. Unique requirements for reactivation of virus-specific memory B lymphocytes. *J. Immunol.* 185: 4011–4021.
 62. Förster, R., A. E. Mattis, E. Kremmer, E. Wolf, G. Brem, and M. Lipp. 1996. A putative chemokine receptor, BLR1, directs B cell migration to defined lymphoid organs and specific anatomic compartments of the spleen. *Cell* 87: 1037–1047.
 63. Rogers, T. F., E. C. Goodwin, B. Briney, D. Sok, N. Beutler, A. Strubel, R. Nedellec, K. Le, M. E. Brown, D. R. Burton, and L. M. Walker. 2017. Zika virus activates de novo and cross-reactive memory B cell responses in dengue-experienced donors. *Sci. Immunol.* DOI: 10.1126/sciimmunol.aan6809.
 64. Trama, A. M., M. A. Moody, S. M. Alam, F. H. Jaeger, B. Lockwood, R. Parks, K. E. Lloyd, C. Stolarchuk, R. Searce, A. Foulger, et al. 2014. HIV-1 envelope gp41 antibodies can originate from terminal ileum B cells that share cross-reactivity with commensal bacteria. *Cell Host Microbe* 16: 215–226.
 65. Williams, W. B., H. X. Liao, M. A. Moody, T. B. Kepler, S. M. Alam, F. Gao, K. Wiehe, A. M. Trama, K. Jones, R. Zhang, et al. 2015. HIV-1 VACCINES. Diversion of HIV-1 vaccine-induced immunity by gp41-microbiota cross-reactive antibodies. *Science* 349: aab1253.